Hydration, Phase Separation and Nonlinear Rheology of Temperature-Sensitive Water-Soluble Polymers

Fumihiko Tanaka*, Tsuyoshi Koga*, Isamu Kaneda†, Françoise M. Winnik‡

*Department of Polymer Chemistry, Graduate School of Engineering, Kyoto University, Kyoto 615-8510, Japan
†Department of Food Science, Rakuno Gakuen University, Ebetsu, Hokkaido 069-8501, Japan
‡Department of Chemistry and Faculty of Pharmacy, University of Montréal, Montréal, Canada H3C 3J7

E-mail: `ftanaka@phys.polym.kyoto-u.ac.jp`

Abstract. Collapse of a poly(*N*-isopropylacrylamide) (PNIPAM) chain upon heating and phase diagrams of aqueous PNIPAM solutions with very flat LCST phase separation line are theoretically studied on the basis of *cooperative dehydration* (simultaneous dissociation of bound water molecules in a group of correlated sequence), and compared with the experimental observation of temperature-induced coil-globule transition by light scattering methods. The transition becomes sharper with the cooperativity parameter σ of hydration. Reentrant coil-globule-coil transition and cononsolvency in mixed solvent of water and methanol are also studied from the viewpoint of *competitive hydrogen bonds* between polymer-water and polymer-methanol. The downward shift of the cloud-point curves (LCST cononsolvency) with the mol fraction of methanol due to the competition is calculated and compared with the experimental data. Aqueous solutions of hydophobically-modified PNIPAM carrying short alkyl chains at both chain ends (*telechelic* PNIPAM) are theoretically and experimentally studied. The LCST of these solutions is found to shift downward along the sol-gel transition curve as a result of end-chain association (*association-induced phase separation*), and separate from the coil-globule transition line. Associated structures in the solution, such as flower micelles, mesoglobules, and higher fractal assembly, are studied by USANS with theoretical modeling of the scattering function. Dynamic mechanical modulus, nonlinear stationary viscosity, stress buildup in start-up shear flows of the associated networks are studied on the basis of the affine and nonaffine transient network theory. The molecular conditions for thickening, strain hardening, stress overshoot are found in terms of the nonlinear amplitude A of the chain tension and the tension-dissociation coupling constant g.

1. Introduction

Aqueous solutions of temperature-sensitive poly(*N*-isopropylacrylamide) (PNIPAM) exhibit flat LCST cloud-point curves at around 32 °C, which are almost independent both of the concentration up to 20 %wt and of the polymer molecular weight[1, 2, 3, 4, 5]. The transmittance of light sharply diminishes in a very narrow temperature region where coil-globule transition (CG transition) of the polymer chain takes place[6]. Sudden change in polymer conformation results in the temperature sensitivity. Although the origin of temperature-sensitivity had long been a mistery, we recently pointed out that it is caused by the cooperative dehydration of the bound water molecules upon heating[7, 8]. On the basis of cooperative hydration, we study (1) sharp CG transition upon heating, (2) LCST with flat cloud point curves, (3) cononsolvency and reentrant CG transition in mixed solvents, (4) shift of LCST by the end-association of hydrophobically modified telechelic PNIPAM, (5) structure of flower micelles and transient gels, and (6) their rheological properties.

2. Temperature-Induced Coil-Globule Transition of PNIPAM Chains and their Phase Separation in Pure Water

The cooperativity in hydration is caused by the positive correlation between neighboring bound water molecules. If a water molecule succeeds in forming a hydrogen bond with an amide group on a chain, a second water molecule can form a bond more easily than the first one because the first molecule causes some displacement of the isopropyl group, which creates more access space for the next molecule. As a result, consecutive sequences of bound water appear along the chain, which leads to a pearl-necklace type chain conformation (Figure 1 [7, 8, 9]). When the chain is heated, each sequence is dehydrated in a group, resulting in the sharp collapse of the chain.

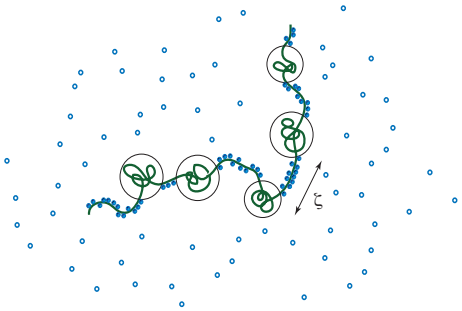

Figure 1. Pearl-necklace conformation induced by the cooperative hydration. Cooperativity originates in the nearest-neighboring bound water molecules. (Printed with permission from [7].)

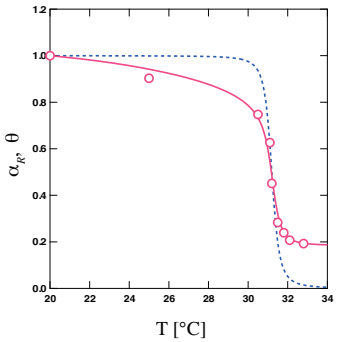

Figure 2. The expansion factor α_R (solid line) and the degree of hydration θ (dotted line) plotted against the temeprature. The expansion factor is compared with the experimental data obtained by Fujishige et al[6]. (Printed with permission from [8].)

Let us first specify the polymer conformation by the index $\mathbf{j} \equiv \{j_1, j_2, \cdots\}$, which indicates that the chain with total number n of repeat units carries the number j_ζ of the hydrated sequences of length ζ (in terms of the number of repeat units). The statistical properties of the chain is described by the canonical partition function

$$Z(T) \equiv \sum_{\mathbf{j}} \exp[-\beta \Delta A(\mathbf{j})] = \sum_{\mathbf{j}} \omega(\mathbf{j}) \prod_{\zeta} (\eta_\zeta)^{j_\zeta} \tag{1}$$

where $\omega(\mathbf{j}) \equiv (n - \sum \zeta j_\zeta)! / \prod j_\zeta! [n - \sum(\zeta + 1) j_\zeta]!$ is the number of different ways to place the hydrated coils and collapsed globules alternatively along the chain. It is related to the entropy of hydration[7, 8]. The weight η_ζ gives the statistical weight for the appearance of the sequence of length ζ. To describe cooperativity, let $-\epsilon$ be the binding free energy of a water molecule, and let $-\Delta\epsilon$ be the interaction energy between the nearest neghboring bound water molecules. Then, it is given by the Zimm-Bragg form[10] $\eta_\zeta = \sigma \eta(T)^\zeta$, where $\sigma \equiv \exp(-\beta \Delta\epsilon)$ is the coopearativity parameter, $\eta(T) \equiv \exp[(\epsilon + \Delta\epsilon)/k_B T]$ is the association constant of the hydrogen bonding. For random hydration, as seen in aqueous solutions of poly(ethylene oxide)s, cooperativity parameter is $\sigma = 1$. Smaller σ gives stronger cooperativity.

Instead of summing up all possible types $\mathbf{j}$, we find the most probable distribution $\mathbf{j}^*$ by minimizing the free energy, by which we calculate the average degree of hydration $\theta(\mathbf{j}^*) \equiv \sum_{\zeta=1}^{n} \zeta j_\zeta / n$ and the mean end-to-end distance $\langle R^2 \rangle$. The latter is normalized by the reference value at 20°C, and is plotted in terms of the expansion factor $\alpha_R \equiv [\langle R^2 \rangle / \langle R^2 \rangle_{(T=20)}]^{1/2}$. Figure 2 compares our calculation with the experimental data[6] of the mean radius of gyration measured by light scattering method. With stronger cooperativity, the transition becomes sharper. Calculation assumes $\sigma = 10^{-4}$ to fit the data. Other fitting parameters are: $n = 7.0 \times 10^4, \lambda_{w0} = 0.001, \gamma_w = 3.788, \Theta = 555, \sigma_w = 2 \times 10^{-5}, \kappa_w = 0.31$.(See Ref.[8] for detailed definition.)

Recent dielectric relaxation measurements give on average 11 water molecules (per PNIPAM monomer) which attach to the chain during the time longer than the dielectric relaxation time (30 ps). Hydration layers around the polymer chain may therefore be multiple, including direct H-bonding to amide groups (1st hydration layer), bridges between the bound water molecules (2nd hydration layer), and outer weakly bound hydrophobic hydration layers. Cooperativity in hydration may be related to the clustering and percolation in these hydration shells[11].

We next consider a model solution in which the number N_1 of polymer chains with n repeat units are mixed with the number N_0 of water molecules. We are based on the lattice-theoretical picture of polymer solutions, and divide the system volume V into cells of size a, each of which can accommodate either a water molecule or a statistical repeat unit of the polymer. We assume incompressibility of the solution, so that we have $\Omega = N_0 + nN_1$, where $\Omega \equiv V/a^3$ is the total number of cells.

To describe adsorption of water, let $N(\mathbf{j})$ be the number of polymer-water (p-w) complexes whose type is specified by the index $\mathbf{j}$ (see Figure 1). The total DP of a complex is given by $n(\mathbf{j}) \equiv n[1 + \theta(\mathbf{j})]$.

Then, the free energy of mixing is given by

$$\beta \Delta F = N_{\rm fw} \ln \phi_{\rm fw} + \sum_{\mathbf{j}} N(\mathbf{j}) \ln \phi(\mathbf{j}) + \beta \sum_{\mathbf{j}} \Delta A(\mathbf{j}) N(\mathbf{j}) + \chi(T) \phi(1-\phi) \Omega \tag{2}$$

where $\phi(\mathbf{j}) \equiv n(\mathbf{j}) N(\mathbf{j}) / \Omega$ is the volume fraction of the complex $\mathbf{j}$, $N_{\rm fw}$ the number of free water molecules in the solution, and $\phi_{\rm fw} \equiv N_{\rm fw}/\Omega$ their volume fraction. $\chi(T)$ is the Flory's interaction parameter for the van der Waals interaction in the background.

$\Delta A(\mathbf{j})$, defined in (1), is the conformational free energy to form a complex of the type $\mathbf{j}$ measured relative to the reference conformation $\mathbf{j}_0 \equiv \{0, 0, \cdots\}$ where no water molecule is adsorbed.

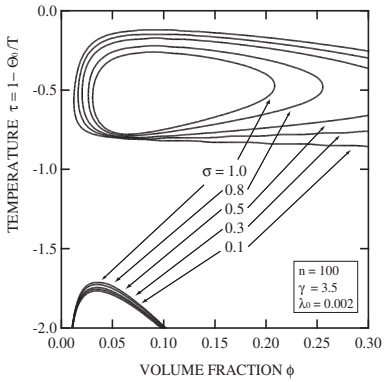

Figure 3. Spinodal lines drawn on the (reduced) temperature and concentration plane for different cooperative parameter σ. (Printed with permission from [7].)

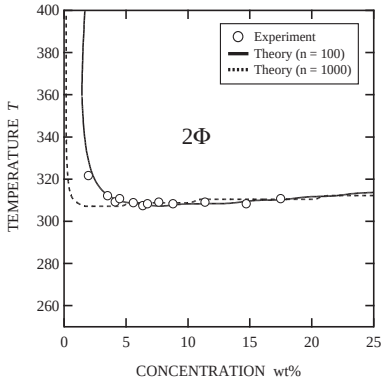

Figure 4. Phase diagrams of aqueous PNIPAM solution. Experimental data (◯) of the spinodal curve is compared with theoretical calculation. The DP of the polymer is $n = 100$(solid line) and $n = 1000$(broken line). (Printed with permission from [7].)

By finding the chemical potentials for the hydrated polymer and water from this free energy, and imposing the hydration equilibrium condition $\Delta\mu(\mathbf{j}) = \Delta\mu(\mathbf{j}_0) + n\theta(\mathbf{j})\Delta\mu_{\rm fw}$, we can study the solution properties such as hydration, phase separation, spinodals. Figure 3 draws the spinodal curves for different cooperative parameter σ with fixed other parameters. It theoretically demonstrates how the bottom part of the miscibility loops become flatter with decrease in σ. In the calculation, usual miscibility domes with UCST appear at low temperature, but these are not observable in the experiments because of the freezing of water.

Figure 4 compares theoretical calculation with experimental data[3] on the spinodal points. In the experiments, the upper part of the miscibility square is impossible to observe because temperature is too high. Theoretical parameters used are $\Theta_0 = 555$ and $\lambda_0 = 0.002$ for $n = 100$, and $\Theta_0 = 565$ and $\lambda_0 = 0.003$ for $n = 1000$. Other parameters are fixed at $\gamma = 3.5, \sigma = 0.3$. (See Ref.[7] for definitions.) The polymer molecular weight used in the experiment is $M_{\rm w} = 615,500$, so that the nominal number of monomers is roughly given by $n = 5,400$. Since the statistical unit used in the lattice theory must be regarded as a group of monomers, we have tried to fit the data by $n = 100$ and 1000. (Theoretical calculation does not depend so much upon the number n if it is larger than 500.) We have seen a good agreement by fixing the cooperative parameter at $\sigma = 0.3$.

3. Reentrant Coil-Globule-Coil Transition and Cononsolvency in Mixed Solvent of Water/Methanol

If methanol is mixed to such aqueous PNIPAM solutions, polymer chain collapses[13], cross-linked gels undergo volume phase transition[14], and polymer solutions phase separate[15, 16], although methanol is a good solvent for PNIPAM. If two good solvents become poor when mixed, they are called *cononsolvents*. In water/methanol mixture, cononsolvency is most evident at around 0.35 mol fraction of methanol. The mixture recovers good solvency at high concentration of methanol. We show here that such a peculiar reentrant behavior of the solutions is caused by the competitive hydrogen bonding of water and methanol onto the polymer chain[8]. The effect becomes strongest where the competition is highest, where the total number of bound molecules shows a minimum.

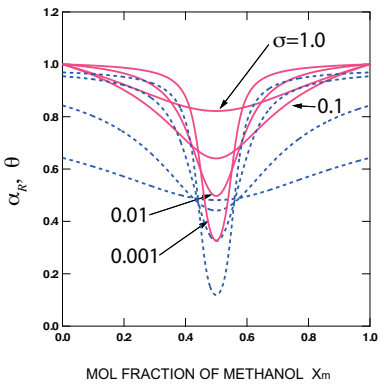

Figure 5. The normalized end-to-end distance (solid lines) and the total coverage by bound molecules (broken lines) are plotted against the molar fraction of the second solvent for the symmetric mixture. The DP of the polymer chain is fixed at $n = 100$. (Printed with permission from [8].)

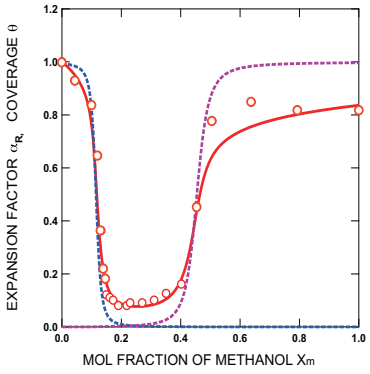

Figure 6. Comparison between the present calculation (line) of the expansion factor for the mean square end-to-end distance for $n = 10^5$ and $p = 2$ and the experimental data of the radius of gyration by Zhang and Wu (circles)[13]. The total coverage is also plotted (broken line). (Printed with permission from [8].)

Figure 5 shows the expansion factor for the end-to-end distance $\alpha_R \equiv [\langle R^2\rangle/\langle R^2\rangle_0]^{1/2}$ (solid lines) and the total coverage $\theta \equiv \theta^{(\mathrm{w})} + \theta^{(\mathrm{m})}$ (broken lines) plotted against the molar fraction x_m of methanol, $\langle R^2\rangle_0$ is the value in pure water. The calculation was done by assuming that all parameters are symmetric and with the metanol/water volume ratio $p = 1$ as a test case. The cooperativity parameter σ varies from curve to curve. We can clearly see that the total coverage takes a minimum value at $x_\mathrm{m} = 0.5$ (stoichiometric concentration) as a result of the competition, so that the end-to-end distance also takes minimum at $x_\mathrm{m} = 0.5$. A slight deviation from stoichiometry is nonlinearly magnified on the chain by cooperativity (*nonlinear*

amplification). As cooperativity becomes stronger, the depression of the end-to-end distance becomes narrower and deeper. A slightest bias in the bulk composition $x_{\rm m}$ from symmetry results in a sharp recovery (*majority rule*). In a real mixture, the association constant and cooperativity parameter are different for water and methanol, so that we expect asymmetric behavior with respect to the molar fraction.

Figure 6 shows a comparison between the experimental mean radii of gyration (circles) obtained by laser light scattering measurements[13] and mean end-to-end distances obtained by theoretical calculations (solid line). Both are normalized by the reference value in pure water. The total coverage θ, including bound water and bound methanol, is also plotted (broken line). The molecular weight of the polymer used in the experiment is $M_{\rm w} = 2.63 \times 10^7$ g mol^{-1}, and hence we fixed $n = 10^5$. The volume ratio is set to be $p = 2$ from the molecular structure of methanol. For larger p, it turned out that the recovery of the expansion factor at high methanol composition was not sufficient. In order to have a sharp collapse at around $x_{\rm m} \simeq 0.17$ we had to fix the cooperativity as high as $\sigma_{\rm w} = 10^{-4}$. Similarly, to produce the gradual recovery at around $x_{\rm m} \simeq 0.4$, we used $\sigma_{\rm m} = 10^{-3}$. The existence of p-w and p-m competition may be detectable experimentally by techniques such as Fourier-transformed infrared spectroscopy.

Theoretical modelling of PNIPAM solutions in mixed solvent of water/methanol was attempted by using three interaction parameters of Flory type[15], but analysis was incomplete; no definite conclusion was drawn due to the unbiguity of their temperature dependence. Similarly to (2), we start from the free energy with competitive hydrogen bonds

$$\begin{aligned}\beta\Delta F &= N_{\rm fw}\ln\phi_{\rm fw} + N_{\rm fm}\ln\phi_{\rm fm} + \sum_{\mathbf{j}_{\rm w}} N(\mathbf{j}_{\rm w})\ln\phi(\mathbf{j}_{\rm w}) + \sum_{\mathbf{j}_{\rm m}} N(\mathbf{j}_{\rm m})\ln\phi(\mathbf{j}_{\rm m}) \\ &+ \beta\sum_{\mathbf{j}_{\rm w},\mathbf{j}_{\rm m}} \Delta A(\mathbf{j}_{\rm w},\mathbf{j}_{\rm m}) N(\mathbf{j}_{\rm w},\mathbf{j}_{\rm m}) + \left[\chi_{\rm pw}\phi_{\rm p}\phi_{\rm w} + \chi_{\rm pm}\phi_{\rm p}\phi_{\rm m} + \chi_{\rm wm}\phi_{\rm w}\phi_{\rm m}\right]\Omega,\end{aligned}$$

Because water and methanol are mixed well to each other, we have $\chi_{\rm wm} = 0$. Also, methanol dissolves PNIPAM at all temperature, we assume $\chi_{\rm pm} = 0$.

Let $\phi_{\rm p} \equiv \phi, \phi_{\rm w} \equiv (1-\phi)(1-v_{\rm m}), \phi_{\rm m} \equiv (1-\phi)v_{\rm m}$ be the volume fraction of PNIPAM, water and methanol, and let $G_{\alpha,\beta} \equiv [\partial\mu_\alpha/\partial\phi_\beta]$ be the Gibbs determinant for the ternary mixture. Figure 7 shows the spinodal lines obtained from the condition for stability limit $|G| = 0$ plotted on the plane of reduced temperature $\tau \equiv 1 - \Theta/T$ and mol fraction of methanol $v_{\rm m}$.The volume fraction of the polymer is fixed at $\phi = 0.1$. We need experimental data in pure methanol to fix the parameters pertaining to methanol, but since they are not available, we fix cooperativity parameter at $\sigma_{\rm m} = 0.3$, and change the amplitude $\lambda_{\rm m0}$ (entropy contribution) in the association constant $\lambda_{\rm m}(T) = \lambda_{\rm m0}\exp[\gamma_{\rm m}(1-\tau)]$. From the miscibility loop in pure water, we have two boundaries (UCST and LCST) which shift downwards with the mol fraction of methanol. The downward shift of the lower boundary from LCST is called *LCST cononsolvency*. Also we have other phase boundary starting from the miscibility dome in pure water (called *UCST cononsolvency*).

Figure 8 magnifies LCST cononsolvency and plot by the real temperature. The minimum of the cloud-point curve depends upon the strength of p-m hydrogen bond, but the initial slopes (proportional to the preferential adsorption coefficient) of the curves are independent of it. In the experiment[15, 16], the temperature drop is the largest, from 31.5 °C down to −7°C, for specific molar fraction $x_{\rm m} = 0.35$ of methanol.

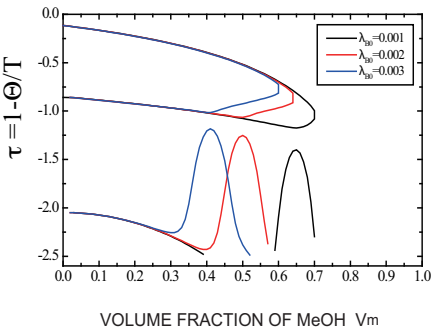

Figure 7. The phase separation region plotted on the reduced temperature-solvent composition plane. The UCST miscibility dome expands sharply in a very narrow region of the volume fraction of methanol. The miscibility loop shifts downward with the methanol volume fraction.

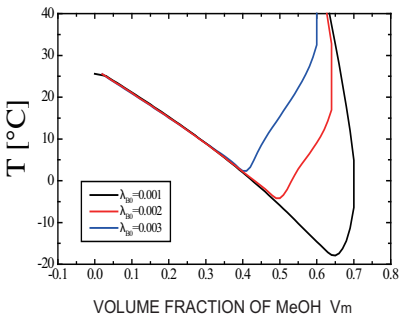

Figure 8. The LCST cononsolvency region is magnified on the temperature-volume fraction plane. The initial slope of the LCST downward shift remains the same for 3 different strength of the methanol hydrogen bonds.

Hence, we can estimate λ_{m0} to be as small as 0.001.

4. Phase Diagrams of Aqueous Solutions of Hydrophobically Modified Telechelic PNIPAMs

The solution properties drastically change when PNIPAM chains are hydrophobically modified. In particular, telechelic PNIPAMs carrying short alkyl chains at their chain ends exhibit a variety of associative structures, from flower micelles to gel networks[19]. In the solutions of telechelic PNIPAM, hydration coexist with end-chain association. The LCST of these solutions is found to decrease along the sol-gel transition line as a result of end-chain association (*association-induced phase separation*).

The LCST deviates from the collapse transition line. We relate the magnitude of the LCST drop to the cooperativity parameter of hydration (Figure 9). The LCST decreases substantially (ca 100 K) in the case of random hydration ($\sigma = 1$ for PEO), whereas only a small shift (ca 5 to 10 K) occurs in the case of cooperative hydration ($\sigma = 0.3$ for PNIPAM). The molecular weight dependence of the LCST curves is inverted; shorter chains show lower LCST (Figure 9). Such an inverted molecular weight dependence is brought by the fact that the number density of the end-chain hydrophobes is larger for the shorter chains when compared at the same weight concentration, and hence tendency for association is stronger for the shorter chains. As a result, the average molecular weight of the aggregates becomes larger, so that the phase separation region expands. Results are compared with experimental observations of the cloud points of tel-PEO and tel-PNIPAM in water.

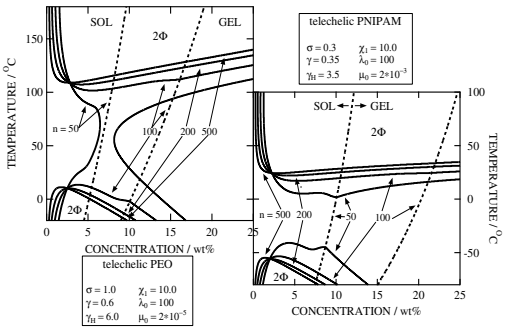

Figure 9. Comparison of the phase diagrams of telechelic associating polymers with random hydration ($\sigma = 1.0$, left) and with cooperative hydration ($\sigma = 0.3$, right). Spinodal lines (solid lines) and sol/gel transition lines (broken lines) are shown.

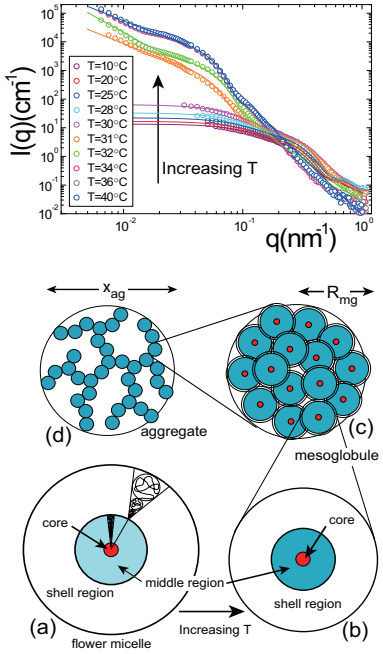

Figure 10. (Top) Neutron scattering intensity of the $c = 10$ g L^{-1} solution of telechelic PNIPAMs ($T = 10 \sim 40$°C) . (a)(b) 3-layered flower micelles, (c) mesoglobules, (d) fractal aggregate of mesoglobules.

5. Solution Structure of Telechelic PNIPAM as studied by Neutron Scattering

On the basis of the results from a small-angle neutron scattering (SANS) study of aqueous solutions of a telechelic PNIPAM with octadecyl end groups, we developed a theoretical model of the self-assembly of this polymer in water as a function of temperature and concentration.

This model leads to the following description (Figure 10). In solutions of concentration 10 gL^{-1} kept between 10 and 20°C, telechelic PNIPAMs ($M_n = 22,200$ g mol^{-1}) associate in the form of flower micelles, containing about 12 polymer chains, assembled in a 3-layered core-shell morphology with an inner core consisting of the octadecyl units, a dense inner shell consisting of partly collapsed PNIPAM chains and an outer shell of swollen hydrated chains. Drastic changes in the scattering profile of the solution heated above 31°C are attributed to the formation of mesoglobules (diameter of ~ 40 nm) consisting of about 1000 polymer chains. On further heating, the aggregation number of the mesoglobules increases. It reaches a value of ~ 9000 at 34°C and stays constant upon further heating.

In solutions of lower concentration (1 gL^{-1}), association of flower micelles and

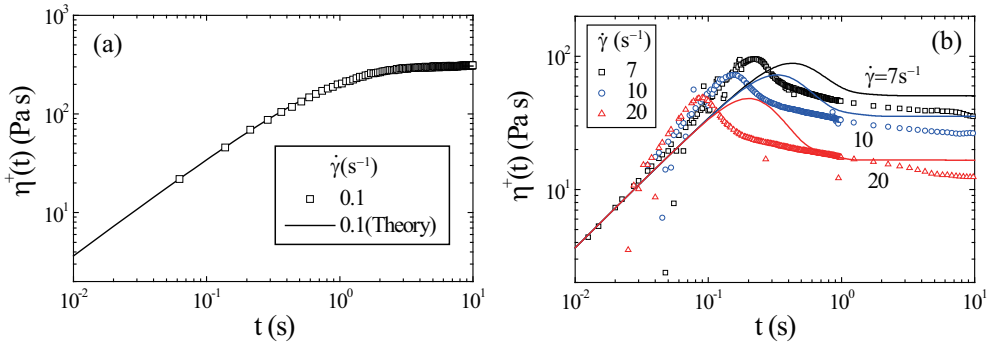

Figure 11. The stress growth function as compared between theory and experiment for a C24-HEUR aqueous solution of 2 wt%. (a) Newtonian regime of small $\dot{\gamma}$, (b) Shear thinning regime of larger $\dot{\gamma}$. (Printed with permission from [22].)

mesoglobules does not occur, however the structure of individual flower micelles and mesoglobules is not affected by the change in concentration. In solutions of 50gL^{-1} in which flower micelles are expected to be partially connected by bridge chains, a peak attributed to correlation between flower micelles appears in the scattering profiles recorded at low temperature ($10 \sim 20$°C). In spite of the intermicellar bridging connection, the overall temperature dependence of the scattering profile at 50 gL^{-1} remains similar to that at 10 gL^{-1}.

6. Rheology of Transient Networks formed by Telechelic PNIPAMs

The nonaffine transient network theory is used to study dynamic-mechanical moduli in networks formed by self-assembled telechelic hydrophobically-modified water-soluble polymers. They behave like a Maxwell fluid with a single relaxation time, but due to the fluctuation and diffusion of the network junctions, the moduli are softened at low frequency region, and tails appear in high-frequency region[20].

The stationary viscosity, 1st and 2nd normal stresses under steady shear flows are also studied on the basis of te affine transient network theory[21]. If the tension of the bridge chains is sufficiently nonlinear ($A > A_c$ in terms of the nonlinear amplitude A of the chain), and if the coupling constant g between the tension and the chain dissociation rate $\beta(\mathbf{r})$ is weak, there is a wide region of the shear thickening on the $A - g$ plane. We numerically show that the first and second normal stress coefficients reveal thickening as a function of shear rate, and that the sign of the second normal stress coefficient changes depending on the nonlinearity in the chain tension, the dissociation rate of the associative groups from junctions, and the shear rate. By analytic calculation, we show that, in the limit of small shear-rate, the sign inversion occurs by the competition between the nonlinear stretching and dissociation of associative groups. Thus, the molecular mechanism of the sign inversion is shown to be similar to that of thickening of the shear viscosity. We also show that thickening of the first normal stress coefficient has a similar molecular origin. The theoretical predictions on thickening of the first normal stress coefficient, and on the positivity of the second normal stress coefficient are confirmed by molecular dynamics simulations of a bead-spring model.

The stress buildup after shear flows with constant shear rates are started are theoretically studied on the basis of the affine transient network model[22]. The initial slope, strain hardening, and overshoot of the shear stress are studied in detail in relation to the nonlinear tension-elongation curve of the elastically active chains in the network. The condition for the occurrence of strain hardening (upward deviation of the stress from the reference curve defined by the linear moduli) is found to be $\dot{\gamma} > \dot{\gamma}_c(A)$, where $\dot{\gamma}$ is the shear rate, $\dot{\gamma}_c$ is its critical value for strain hardening, and A is the amplitude of the nonlinear term in the tension of a chain. The critical shear rate $\dot{\gamma}_c$ is calculated as a function of A. It is approximately 6.3 (in the time unit of the reciprocal thermal dissociation rate) for a nonlinear chain with $A = 10$. The overshoot time $t_{\max}$ when the stress reaches a maximum, and the total deformation $\gamma_{\max} \equiv \dot{\gamma} t_{\max}$ accumulated before the peak time are obtained in terms of the molecular parameters of the polymer chain. The maximum deformation $\gamma_{\max}$ turns out to depend weakly upon the shear rate $\dot{\gamma}$. The first and second normal stress differences are also studied on the basis of the exact numerical integration of the theoretical model paying special attention on their overshoot, undershoot, and sign change as a function of the shear rate. These theoretical results are compared with recent rheological experiments of the solutions of telechelic hydrophobically modified poly(ethylene oxide)s carrying short branched alkyl chains (2-decyl-tetradecyl) at both ends.

acknowledgements This work is partly supported by a Grant-in-Aid for Scientific Research on Priority Areas "Soft Matter Physics" from the Ministry of Education, Culture, Sports, Science and Technology of Japan, and partly supported by a Grant-in-Aid for Scientific Research (B) from the Japan Society for the Promotion of Science under grant number 19350057. We wish to acknowledge their support.

References

[1] Schild, H. G. *Prog. Polym. Sci.* **1992**, *17*, 163; Heskins, M.; Guillet, J. E. *J. Macromol. Sci. - Chem.* **1968**, *A2*, 1441.
[2] Afroze, F.; Nies, E.; Berghmans, H. *J. Molecul. Str.* **2000**, *554*, 55.
[3] de Azevedo, R. G.; Rebelo, L. P. N.; Ramos, A. M.; Szydlowski, J.; de Sousa, H. C.; Klein, J. *Fluid Phase Eq.* **2001**, *185*, 189.
[4] Rebelo, L.P.N.; Visak, Z.P.; de Sousa,. HC.; Szydlowski, J.; de Azevedo, R.G.; Ramos, A.M.; Najdanovic-Visak, V.; da Ponte, M.N.; Klein, J. *Macromolecules* **2002**, *35*, 1887.
[5] Milewska, A.; Szydlowski, J.; Rebelo, L. P. N. *J. Polym. Sci., Part B: Polym. Phys.* **2003**, *41*, 1219.
[6] Fujishige, S.; Kubota, K.; Ando, I. *J. Phys. Chem.* **1989**, *93*, 3311.
[7] Okada, Y.; Tanaka, F. *Macromolecules* **2005**, *38*, 4465.
[8] Tanaka, F.; Koga, T.; Winnik, F. M. *Phys. Rev. Lett.* **2008**, *101*, 028302; Tanaka, F.; Koga, T.; Kojima, H.; Winnik, F. M. *Macromolecules* **2009**, *42*, 1321.
[9] Ye, X.; Lu, Y.; Shen, L.; Ding, Y.; Liu, S.; Zhang, G.; Wu, C. *Macromolecules* **2007**, *40*, 4750.
[10] Zimm, B. H.; Bragg, J. K. *J. Chem. Phys.* **1959**, *31*, 526.
[11] Brovchenko, I.; Krukau, A.; Smolin, N.; Oleinikova, A.; Geiger, A.; Winter, R. *J. Chem. Phys.* **2005**, *123*, 224905.
[12] Balu, C.; Delsanti, M.; Guenoun, P. *Langmuir* **2007**, *23*, 2404.
[13] Zhang, G.; Wu, C. *J. Am. Chem. Soc.* **2001**, *123*, 1376.
[14] Hirotsu, S. *J. Chem. Phys.* **1988**, *88*, 427.
[15] Schild, H. G.; Muthukumar, M.; Tirrel, D. A. *Macromolecules* **1991**, *24*, 948.
[16] Winnik, F. M.; Ottaviani, M. F.; Bossmann, S. H.; Garcia-Garibay, M.; Turro, N. J. *Macromolecules* **1992**, *25*, 6007; Winnik, F. M.; Ottaviani, M. F.; Bossmann, S. H.; Pan, W.; Carcia-Gaibay, M.; Turro, N. J. *Macromolecules* **1993**, *26*, 4577.
[17] Okada, Y.; Tanaka, F.; Kujawa, P.; Winnik, F. M. *J. Chem. Phys.* **2006**, *125*, 244902.
[18] Kujawa, P.; Aseyev, V.; Tenhu, H.; Winnik, F. M. *Macromolecules* **2006**, *39*, 7686.

[19] Koga, T.; Tanaka, F.; Motokawa, R.; Koizumi, S.; Winnik, F. M. *Macromolecules* **2008**, *41*, 9413.
[20] Tanaka, F.; Koga, T. *Macromolecules* **2006**, *39*, 5913.
[21] Koga, T.; Tanaka, F. *Macromolecules* **2010**, *43*, 3052.
[22] Koga, T.; Tanaka, F.; Kaneda, I.; Winnik, F. M. *Langmuir* **2009**, *25*, 8626.